# Preparation of Thin Silica Films with Controlled Thickness and Tunable Refractive Index

Jason H. Rouse and Gregory S. Ferguson*

*Contribution from the Departments of Chemistry and Materials Science & Engineering, Lehigh University, Bethlehem, Pennsylvania 18015-3172*

Received May 20, 2003;  E-mail: gf03@lehigh.edu.

**Abstract:** Silica films with controlled thickness and refractive index have been formed by the sequential adsorption of a cationic polyelectrolyte and silica sols. The conditions used to prepare the sol were varied, and allowed films with refractive indices as low as 1.16 to be obtained. The sequential adsorption technique allows the thickness of these films to be controlled in increments of 5−10 nm, depending on the desired refractive index. Scanning electron microscopy revealed that a low packing density of constituent silica particles was responsible for the low indices of these films. The as-adsorbed films are thermally robust; calcination at 500 °C resulted in only very small decreases in film thickness (by ≤1.8%) and refractive index (to as low as 1.14). After calcination, the silica films remained hydrophilic and sorbed water vapor from the atmosphere. As a result, the refractive indices of these films increased with increasing relative humidity (RH). The dependence of the refractive index on RH was eliminated by treating the calcined films with trimethylchlorosilane.

## Introduction

Porous silica films are currently of technological interest in applications ranging from low-dielectric constant ("low-*k*") materials[1−6] to antireflective coatings[7,8] to molecular separations.[9−12] Standard routes to these materials include the chemical vapor deposition (CVD) of silicon oxide precursors[8] and the spin- or dip-coating of partially hydrolyzed silicon alkoxide solutions, i.e., sol−gel chemistry.[13] Depending on the processing conditions used in sol−gel chemistry, the porsity of resulting films can be controlled. For example, films can be allowed to condense during removal of the solvent to form a material of low-to-medium porosity (xerogel), or they can first be treated with organosilanes prior to solvent removal to produce porosities of up to 99.9% (aerogel).[1] Here, we report a method utilizing an unmodified sol to produce films with porosities ranging from 30% to 67% and with a high degree of control over film thickness. This simultaneous control of both parameters is important because it fully defines the optical path length within the resulting films.

Our method for forming porous films relies on the adsorption of polyionic species onto a surface of opposite charge, a technique reported initially by Iler in the mid 1960s[14] that has attracted a great deal of interest more recently.[15,16] We have found that oligomeric silica species can be adsorbed from sols derived from tetraethyl orthosilicate (TEOS) onto substrates bearing a very thin (∼6 Å) layer of positively charged polyelectrolyte. Furthermore, by varying the conditions used to prepare the sol, robust films can be prepared with refractive indices in the range of 1.16−1.31. Although others have reported adsorptions of larger particles of *colloidal* silica,[14,17] the molecular sol−gel method reported here allows not only nanometer control of film thickness but also unprecedented control of the amount of porosity within these films.

(1) Prakash, S. S.; Brinker, C. J.; Hurd, A. J.; Rao, S. M. *Nature* **1995**, *374*, 439. Prakash, S. S.; Brinker, C. J.; Hurd, A. J. *J. Non-Cryst. Solids* **1995**, *190*, 264.
(2) Zhao, D.; Feng, J.; Huo, Q.; Melosh, N.; Fredrickson, G. H.; Chmelka, B. F.; Stucky, G. D. *Science* **1998**, *279*, 548. Zhao, D.; Yang, P.; Melosh, N.; Feng, J.; Chmelka, B. F.; Stucky, G. D. *Adv. Mater.* **1998**, *10*, 1380.
(3) Hguyen, C.; Hawker, C. J.; Miller, R. D.; Huang, E.; Hedrick, J. L.; Gauderon, R.; Hilborn, J. G. *Macromolecules* **2000**, *33*, 4281. Nguyen, C. V.; Carter, K. R.; Hawker, C. J.; Hedrick, J. L.; Jaffe, R. L.; Miller, R. D.; Remenar, J. F.; Rhee, H.-W.; Rice, P. M.; Toney, M. F.; Trollsas, M.; Yoon, D. Y. *Chem. Mater*. **1999**, *11*, 3080. Hedrick, J. L.; Miller, R. D.; Hawker, C. J.; Carter, K. R.; Volksen, W.; Yoon, D. Y.; Trollsas, M. *Adv. Mater.* **1998**, *10*, 1049.
(4) Doshi, D. A.; Huesing, N. K.; Lu, M.; Fan, H.; Lu, Y.; Simmons-Potter, K.; Potter, B. G., Jr.; Hurd, A. J.; Brinker, C. J. *Science* **2000**, *290*, 107.
(5) Baskaran, S.; Liu, J.; Domansky, K.; Kohler, N.; Xiahong, L.; Coyle, C.; Fryxell, G. E.; Thevuthasan, S.; Williford, R. E. *Adv. Mater.* **2000**, *12*, 291. Jin, C. M.; Luttmar, J. D.; Smith, D. M.; Ramos, T. A. *Mater. Res. Soc. Bull*. **1997**, *22*, 39.
(6) Nguyen, S. V. *IBM J. Res. Dev.* **1999**, *43*, 109.
(7) Uhlmann, D. R.; Suratwala, T.; Davidson, K.; Boulton, J. M.; Toewee, G. *J. Non-Cryst. Solids* **1997**, *218*, 113.
(8) Martinu, L.; Poitras, D. *J. Vac. Sci. Technol. A* **2000**, *18*, 2619.
(9) de Vos, R. M.; Maier, W. F.; Verweij, H. *J. Membr. Sci.* **1999**, *158*, 277. de Vos, R. M.; Verweij, H. *J. Membr. Sci.* **1998**, *143*, 37. de Vos, R. M.; Verweij, H. *Science* **1998**, *279*, 1710.
(10) Yang, H.; Coombs, N.; Sokolov, I.; Ozin, G. A. *Nature* **1996**, *381*, 589.
(11) Lu, Y.; Ganguli, R.; Drewien, C. A.; Anderson, M. T.; Brinker, C. J.; Gong, W.; Guo, Y.; Soyez, H.; Dunn, B.; Huang, M. H.; Zink, J. I. *Nature* **1997**, *389*, 364.
(12) Cot, L.; Ayral, A.; Durand, J.; Guizard, C.; Hovnanian, N.; Julbe, A.; Larbot, A. *Solid State Sci.* **2000**, *2*, 313.
(13) Brinker, C. J.; Scherer, G. W. *Sol−Gel Science: The Physics and Chemistry of Sol−Gel Processing*; Academic Press: New York, 1990.
(14) Iler, R. K. *J. Colloid Interface Sci.* **1966**, *21*, 569.
(15) Kleinfeld, E. R.; Ferguson, G. S. *Science* **1994**, *265*, 370.
(16) Decher, G.; Hong, J. D. *Ber. Bunsen-Ges. Phys. Chem.* **1991**, *95*, 1430. Keller, S. W.; Kim, H.-N.; Mallouk, T. E. *J. Am. Chem. Soc.* **1994**, *116*, 8817. For a review of stepwise multilayer self-assembly techniques, see: Decher, G. *Science* **1997**, *277*, 1232.

## Results and Discussion

**Synthesis and Characterization of Polyelectrolyte/Silica Films.** Sols were prepared by first allowing an aqueous solution of TEOS (0.01 M) to stir for 2 h. A sufficient amount of aqueous sodium hydroxide was then added to produce either a 35:1 (sol A) or a 175:1 (sol B) molar ratio of TEOS to base. The corresponding initial concentrations of base in these solutions were ∼0.28 mM and ∼0.057 mM for sol A and sol B, respectively. The resulting solution was allowed to age stirring until use. A third sol (sol C) was prepared by adding the TEOS directly to aqueous sodium hydroxide to produce a 0.01 M TEOS solution having an initial 175:1 molar ratio of TEOS to base. This solution was also stirred until use. Substrates used for film formation were rectangular (100)-oriented silicon wafers bearing a hydroxylated native-oxide surface, with a size of ∼1 cm by 3.5 cm. To form a film, the substrate was dipped into a 0.25% (w/w) aqueous solution of poly(diallydimethylammonium chloride) (PDDA) for 3 min, then removed, rinsed with deionized water, and dried with nitrogen. After it was rinsed and dried a second time, the film was placed into a stirred, aqueous TEOS sol for 3 min. The rinsing and drying procedure was then repeated. In the following discussion, a treatment with PDDA followed by one with a TEOS sol constitutes a single "adsorption cycle."

The choice of 3-min adsorption times resulted from the following kinetics experiments for adsorptions performed using sols A and B. Substrates were pretreated with two adsorption cycles using 0.25% (w/w) PDDA and the sol of interest, with a ∼15-s adsorption time for each component. This priming step was meant to minimize any substrate effects in the kinetics experiments. Films were then adsorbed onto the pretreated substrates from 0.25% (w/w) PDDA and the sol of interest for various amounts of time—5 s, 15 s, 30 s, 1, 3, or 10 min—with the same adsorption time used for both the PDDA and the sol. For the shortest treatment times (5, 15, and 30 s), the component solutions were pipetted onto the substrate surface; for the longer treatments, the substrate was immersed into the component solutions.

Because the composition of a sol depends on the length of time it has aged,[13] kinetic data were obtained not only as a function of adsorption time but also as a function of the age of the sol (i.e., 1 d, 2 d, etc.). Adsorption data obtained for sol A are shown in Figure 1a. Each data point corresponds to the average of three measurements taken on a particular sample, and a separate sample was used for each point. The data show that a region of slow growth in the amount adsorbed is not reached until at least ∼3 min of adsorption time, and that for sols aged between 1 and 3 d, the amount adsorbed at the steady-state was reproducible.

Analogous kinetics experiments performed with sol B are shown in Figure 1b. Unlike sol A, from which adsorption was detected after only 1 d of aging, no adsorption of silica from sol B was found until the sol had aged for at least 3 d. For a sol aged for 3 days, a plateau in growth was reached after 3 min of adsorption time, and for sols aged for longer amounts of time (i.e., 5, 7, and 9 d), an approximate plateau was reached after
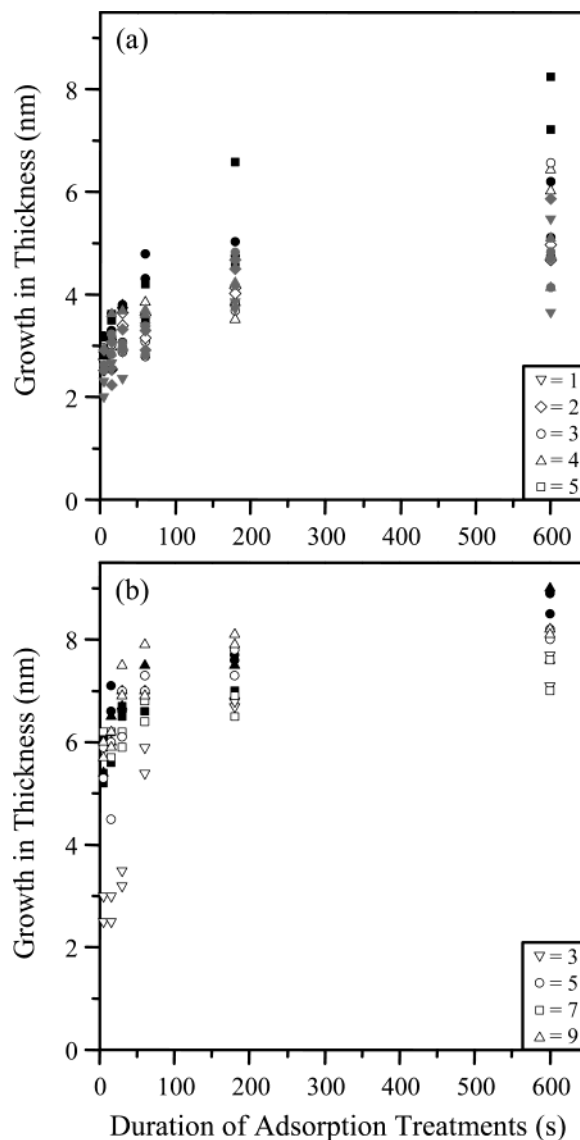
(17) Lvov, Y. M.; Rusling, J. F.; Thomsen, D. L.; Papadimitrikopoulos, F.; Kawakami, T.; Kunitake, T. *Chem. Commun.* **1998**, 1229. Lvov, Y.; Ariga, K.; Onda, M.; Ichinose, I.; Kunitake, T. *Langmuir* **1997**, *13*, 6195. Ariga, K.; Lvov, Y.; Onda, M.; Ichinose, I.; Kunitake, T. *Chem. Lett.* **1997**, 125.

**Figure 1.** Dependence of film growth on the duration of the adsorption treatments with 0.25% (w/w) PDDA and either sol **A** (a) or sol **B** (b). The same adsorption time was used for each component, and each point corresponds to a single sample (two for each adsorption time). The shape of the symbol indicates the age of the sol in days (see legend), and the shading of the symbol represents samples prepared from the same batch of sol. Substrates for this study were silicon wafers that had been pretreated with two cycles of PDDA and the sol studied (15-s adsorption times). All thicknesses were calculated assuming a refractive index of 1.30 for films prepared with sol **A**, and a refractive index of 1.25 for those prepared with sol **B**.

only 1 min. In the regime of slower growth (the "plateau"), the average adsorbed amount was approximately 70% greater than for sol A. Given that a 3-min adsorption time was sufficient to reach the regime of slow growth for both sols, we chose that amount of time for the preparation of films from all three sols examined in this study.

Optical ellipsometry was used both to monitor the growth in thickness of the sequentially adsorbed films and to determine the refractive index of films having a thickness greater than ∼80 nm.[18] As an example, growth data obtained for sol A are shown in Figure 2a. All of the ellipsometric measurements were

(18) Tompkins, H. G. *A User's Guide to Ellipsometry*; Academic Press: Boston, 1993, Chapters 1−3.

**Figure 3.** Survey XPS spectra of a multilayer film formed from PDDA and sol **A**: (a) as-adsorbed, (b) after heating at 500 °C in air for 10 h, and (c) after treatment with trimethylchlorosilane (vide infra).
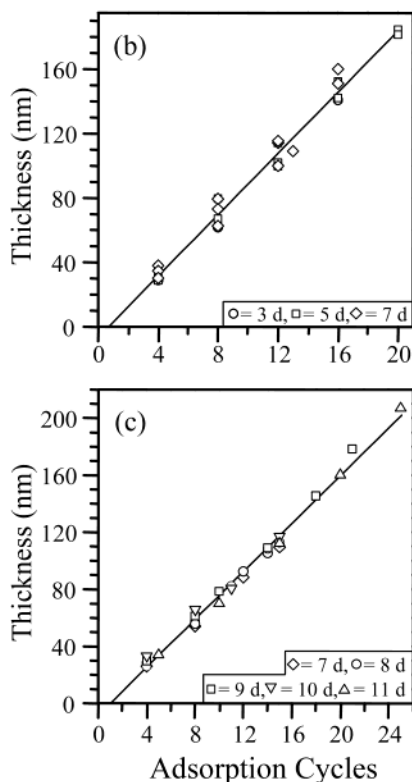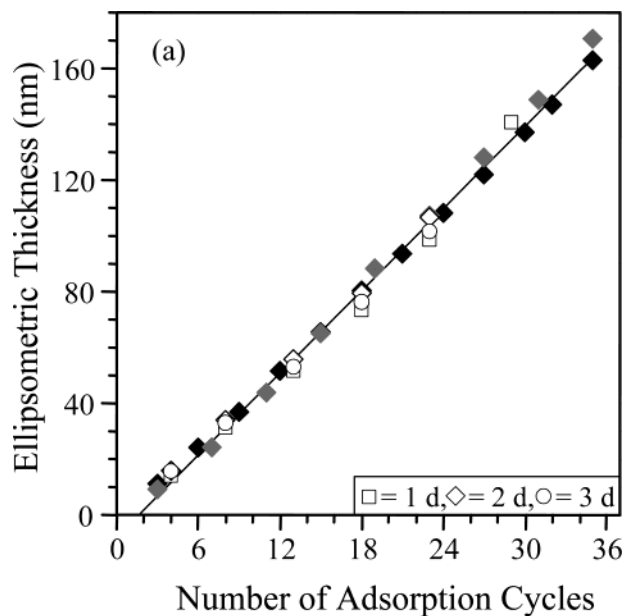
**Figure 2.** (a) Increase in ellipsometric thickness of multilayer films formed from 0.25% (w/w) PDDA and sol **A** as a function of the number of adsorption cycles and age of the sol. The shading of the symbols indicates films prepared from the same batch of sol, and the shape of symbol indicates the number of days the sol was aged (see legend). (b and c) Analogous data obtained for sols **B** and **C**. For clarity, data for films from all batches of sol were plotted using the same color. The lines are linear least-squares fits to all of the data. Film thicknesses for all three graphs were calculated using the refractive index determined for each individual film, a range of 1.29−1.31, 1.24−1.26, and 1.16−1.18, for sols **A**, **B**, and **C**, respectively.

taken with the sample under nitrogen at a relative humidity of 4−7% to minimize the effect of sorption of ambient water vapor within these hydrophilic films (vide infra). Because the composition of a sol depends on the length of time it has aged, films were produced from three different batches of sol and
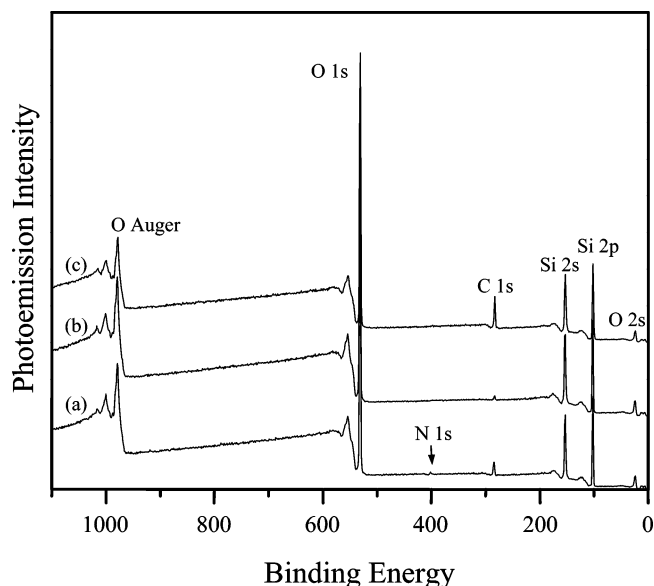
after various aging times (1−3 d, as noted). These sols produced nearly identical linear growth rates, indicating the reproducibility of both the sol formation and adsorption characteristics over 1 to 3 d. A linear fit to all of the data gave an average growth per cycle of 4.7 ± 0.1 nm, consistent with that determined from the data in Figure 1a. The refractive indices of these films were in the range of 1.29−1.31, values significantly lower than that of bulk silica (∼1.46).[19]

Increasing the molar ratio of TEOS to base from 35:1 to 175:1 (sol B) gave films having refractive indices of 1.24−1.26. Films prepared from four different batches of sol and analyzed after various days of aging gave reproducible day-to-day and batch-to-batch growth (Figure 2b). The average growth per cycle roughly doubled from that found for sol A, to 9.5 ± 0.3 nm. This value is slightly higher than that determined from the data in Figure 1b. Using the same 175:1 molar ratio of TEOS to base, but with the TEOS added directly to the base solution (sol C), gave films with even lower refractive indices, 1.16−1.18. Longer aging times were needed for this sol: no growth occurred until the sol had aged for at least 6 d, and uniform films resulted only after the sol had aged for at least 7 d. The average growth per cycle for films prepared from three batches of sol C that had aged for between 7 and 11 d was 8.4 ± 0.3 nm (Figure 2c).

To determine the relative amounts of PDDA and silica incorporated within these films, the outer surface of a film was analyzed by X-ray photoelectron spectroscopy (XPS). Survey spectra at a 90° takeoff angle between the detector and the sample surface revealed that the interfacial region of both films contained oxygen, silicon, carbon, and nitrogen, as expected. The survey spectrum obtained from the film prepared from sol A is shown in Figure 3a. High-resolution spectra (also at a 90° takeoff angle) of the film prepared from sol A revealed mostly oxygen (59.1%) and silicon (33.6%), with a small amount of carbon (6.7%) and very little nitrogen (0.6%). After accounting

(19) *Handbook of Chemistry and Physics,* 73rd ed.; Lide, D. R., Ed.; CRC Press: Boca Raton, Florida, 1992; pp 4−95.

for the amount of carbon and nitrogen associated with the PDDA, based on the nitrogen 1s photoemission, we calculate the amount of excess carbon to be only 1.9%. If the excess carbon were all due to unhydrolyzed ethoxy groups of the TEOS, it would represent ~98% hydrolysis of the ethoxy-silicon groups. With the film containing only ~5.4% PDDA "glue", the ~4.7 nm growth per cycle can be almost completely attributed to the adsorbed silica. For comparison, a film prepared from sol C was also analyzed by XPS and contained 5.6% carbon and only 0.6% nitrogen.

The thickness and refractive index across the surfaces of all of these films were remarkably even: the average of four measurements across the films always agreed to within ±2%. A consequence of the uniformity in the optical path length of these films was a uniform color across each film due to interference of visible light reflected from the air-film interface with that reflected from the film−substrate interface.[15,20] Neither the sol nor the polyelectrolyte contain a chromophore. The refractive index of the film affected the intensity of this interference color: as the refractive index decreased, the color became fainter, presumably due to less light being reflected from the air−film interface. The interference wavelength was also slightly blue-shifted in films of lower index.

The volume fraction of air within such a material can be estimated from its refractive index, according to the Lorentz−Lorenz relationship[13,21]

$$(n_f{}^2 - 1)/(n_f{}^2 + 2) = (1 - V_p)(n_s{}^2 - 1)/(n_s{}^2 + 2) \quad (1)$$

where $n_f$ is the refractive index of the film, $V_p$ is the void volume fraction, and $n_s$ is the refractive index of the void-free solid framework. Given the absence of crystalline structure within these films (absence of Bragg peaks in X-ray diffractograms), the index of amorphous silica (1.46) was assumed for the void-free framework here. From eq 1, as the index of the films decreased from 1.30 ± 0.1 (sol A) to 1.25 ± 0.1 (sol B) to 1.17 ± 0.1 (sol C), the $V_p$ increased from 0.31 ± 0.02 to 0.40 ± 0.2 to 0.60 ± 0.01, respectively.

To understand how the porosity is incorporated within these films, the morphology of a film prepared from each sol was analyzed by scanning electron microscopy (SEM). Low-magnification images of the surface of all three of the films showed a very uniform coating of small (~100 nm) particles, with no cracks or other imperfections present (Figure 4a, b, and c). At higher magnification (Figure 4d, e, and f), however, significant differences in topography are evident. The packing density of the particles was clearly lower for the films of lower refractive index, indicating that the low refractive index of these films is due to an increased amount of interparticle void space.

Additional evidence for the variation in film structure from sol-to-sol was provided by cross-sectional SEM. Again, the film prepared from sol C (Figure 5c) showed a more diffuse structure than those prepared from either sol A (Figure 5a) or sol B (Figure 5b). Higher resolution micrographs (Figure 6) of the film prepared from sol C clearly shows that the ~100-nm particles in Figure 4e are actually aggregates of smaller (~10-
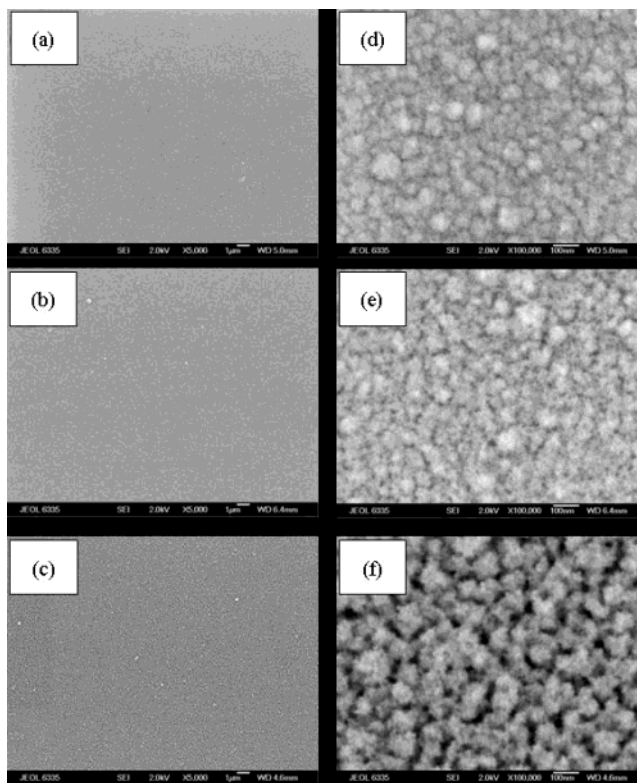


**Figure 4.** Top-down scanning electron micrographs (SEM) of as-adsorbed films prepared from sol **A** (a and d), sol **B** (b and e), and sol **C** (c and f). The scale bars in micrographs a−c are 1 $\mu$m in length (5000 magnification), and in d−f are 100 nm in length (100 000 magnification).

nm) particles, a morphology similar to that of silica aerogels.[22] Consistent with the large void volume present in films prepared from sol C, an XPS spectrum (90° takeoff angle) revealed photoemission from *elemental* silicon (2p) of the substrate on a sample bearing a 119-nm overlayer film! All three films examined by SEM had uniform thicknesses consistent with those values determined by ellipsometry: the SEM thicknesses were within 10% of the ellipsometric thicknesses. The close correspondence of the SEM and ellipsometric thicknesses is critical because it confirms the ellipsometric analyses that yielded the low refractive indices for these films.

Taken together, the SEM and XPS results indicate that the films prepared from sol C contain void space throughout the layer. To verify that the pores were not continuous, SEM images were collected, while progressively increasing the electron-accelerating voltage, thus allowing the electron beam to interact with a larger volume of the material—the interaction volume—and probe progressively deeper into the film (Figure 7).[23] As the accelerating voltage was increased, the amount of void space appeared to decrease and be replaced with a morphology similar to that of the upper surfaces. We infer from these micrographs that at low accelerating voltage, the number of secondary electrons emitted from within the "void spaces" and reaching the detector was lower than the contrast level set for image

(20) Decher, G.; Hong, J. D.; Schmitt, J. *Thin Solid Films* **1992**, *210/211*, 831. Tillman, A.; Ulman, A.; Penner, T. L. *Langmuir* **1989**, *5*, 101. Pliskin, W. A.; Conrad, E. E. *IBM J. Res. Dev.* **1964**, *8*, 43. Blodgett, K. B. *J. Am. Chem. Soc.* **1935**, *57*, 1007.
(21) Born, M.; Wolf, E. *Principles of Optics*; Pergamon: New York, 1980; pp 87−88.

(22) Ruffner, J. A.; Clem, P. G.; Tuttle, B. A.; Brinker, C. J.; Sriram, C. S.; Bullington, J. A. *Thin Solid Films* **1998**, *332*, 356. Loy, D. A.; Russick, E. M.; Yamanaka, S. A.; Baugher, B. M.; Shea, K. J. *Chem. Mater.* **1997**, *9*, 2264. Ruben, G. C.; Hrubesh, L. W.; Tillotson, T. M. *J. Non-Cryst. Solids* **1995**, *186*, 209.
(23) Goldstein, J. I.; Newbury, D. E.; Echlin, P.; Joy, D. C.; Romig, A. D.; Lyman, C. E.; Fiori, C.; Lifshin, E. *Scanning Electron Microscopy and X-ray Microanalysis: Text for Biologists, Materials Scientists, and Geologists*; Plenum Press: New York, 1992, Chapters 3 and 4.
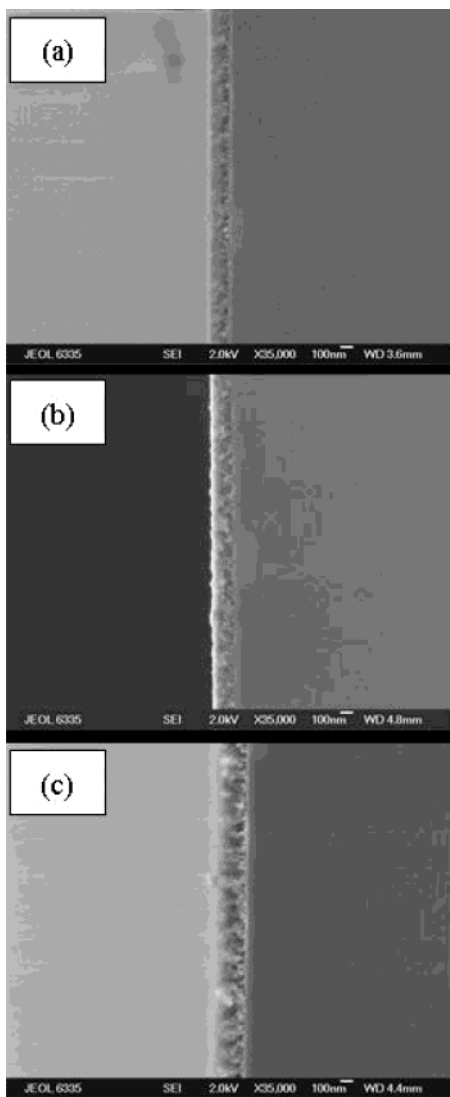
**Figure 5.** Cross-sectional SEM micrographs of the same films imaged in Figure 4: sol **A** (a), sol **B** (b), and sol **C** (c). The scale bars in these micrographs are 100 nm in length (35 000 magnification). The substrates (right side) in these images are silicon wafers.



**Figure 6.** (top) High-magnification top-down SEM of the same film imaged in Figure 4c and f (sol **C**) and (bottom) a high-magnification-*cross*-sectional SEM of the same film. Images were obtained on a JEOL 6700 FESEM.

display.[23] Images are normally displayed by setting the dynamic range of the display such that the lowest signal level is just above that of black and the highest signal level is just below that of white (i.e., no saturation of signal). For these images, the contrast levels were set individually. Therefore, as the accelerating voltage was increased, the signal from the void spaces was of sufficient intensity to register as gray.

**Effect of Relative Humidity and Post-treatment on the Refractive Index and Thickness of the Films.** To remove the small amount of PDDA and residual ethoxy groups present within these films, they were heated at 500 °C in air for 10 h. X-ray photoelectron spectroscopy showed that this calcination resulted in a decrease in the amount of carbon present in a film formed from sol A from 6.7 % to only 1.5 % (survey spectra shown in Figure 3b). The corresponding reduction for a film formed from sol C was from 5.5 % to only 1.4 %. For both films, the nitrogen was completely eliminated to the limit of the sensitivity of the measurement.[24] Consistent with the removal

---

(24) Single films from sols A and C were cut into samples for XPS analysis of both the calcined and uncalcined states.
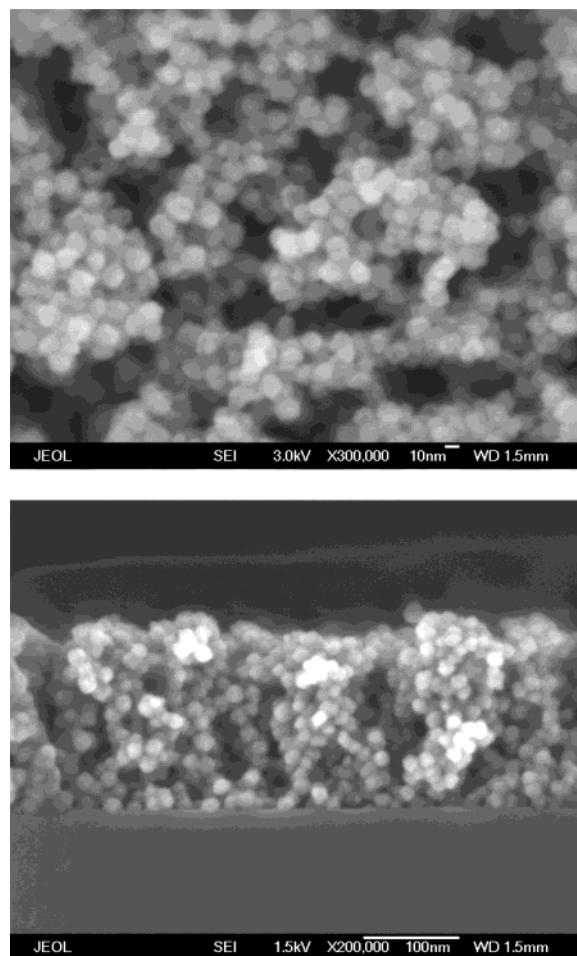
of residual organic material, the refractive indices of the films decreased upon calcination, allowing films with indices as low as 1.14 ($V_p$ of 67%) to be formed! The refractive index of films from sol A fell from $1.30-1.31$ to $1.26-1.27$; those from sol B fell from $1.24-1.26$ to $1.21-1.23$; and those from sol C fell from $1.15-1.17$ to $1.14-1.16$. The steeper decrease in index for films prepared with sol A, compared to sol C, is consistent with the former initially having more organic content. The robustness of the films was evidenced by a mere $\sim$1.8%, or less, reduction in film thickness in all cases upon calcination.

As the relative humidity (RH) was increased from 3 to 70%, the refractive index of the as-adsorbed films also increased, with the magnitude of the response scaling roughly with the refractive index at low-RH (Figure 8). Increasing the humidity from 3 to 70% caused an increase in index of $\sim$0.09 for films prepared with sol A, versus $\sim$0.07 and $\sim$0.05 for film prepared with sol B and C, respectively. Nearly identical results were found using a second film prepared from each of the three sols. The larger effect of relative humidity on films prepared with sol A is consistent with the SEM study showing that those films comprise a denser packing of $\sim$10 nm silica particles than films from either sol B or sol C. As the packing density of particles increases, the amount of hydrophilic surface area capable to absorb water would also increase in these porous solids.

Although calcination caused the refractive index of films prepared from each sol to decrease, it only affected the RH
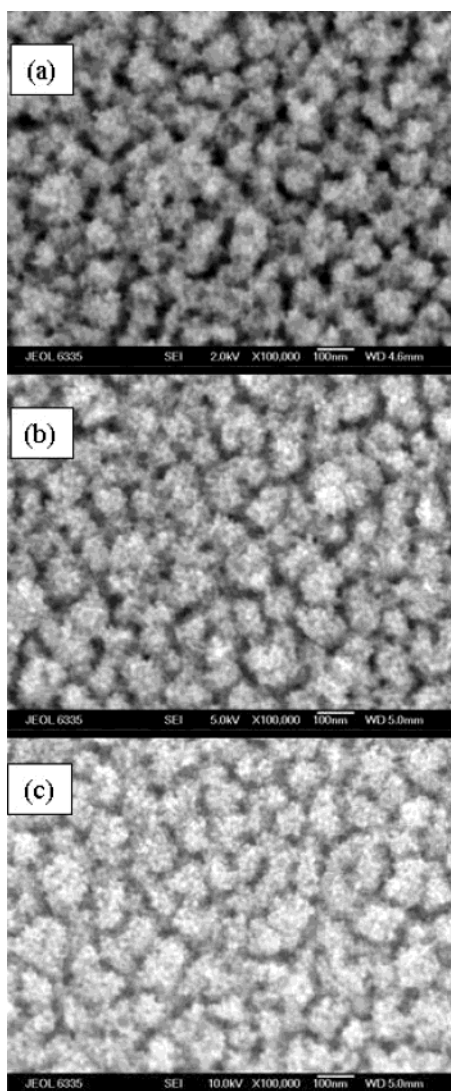
**Figure 7.** Scanning electron micrographs obtained at different accelerating voltages of a film prepared from sol **C**: (a) 2 kV, (b) 5 kV, and (c) 10 kV. The scale bars in these micrographs are 100 nm in length (100 000 magnification).



**Figure 8.** Refractive index as a function of relative humidity (RH) for films prepared with sol **A** (a), sol **B** (b), and sol **C** (c): as-absorbed (squares); after calcination at 500 °C for 10 h (circles); and after treatment with trimethylchlorosilane (diamonds). The open symbols represent data obtained with increasing RH, and the filled symbols were obtained with decreasing RH. The lines drawn are guides for the eye. Note that the y-axes on these graphs show different ranges.

response of films prepared from sol B (Figure 8b). Films prepared with sol B had an average 50% reduction in the magnitude in refractive index response in going from 3 to 70% RH, compared to the as-adsorbed data. For films prepared with sols A and C, the respective curves were only shifted to lower values but the magnitude of the response did not appear to be effected. This insensitivity of the humidity response indicates that either the calcination temperature was insufficient to cause condensation of silanol groups or that the structure within the films hindered such condensation. Despite the changes in the indices of these films with RH, their thicknesses remained nearly constant, to within the experimental error associated with the measurement, indicating that both the as-adsorbed and calcined films are rigid frameworks.

Treatment of the calcined films with trimethylchlorosilane (TMSCl) vapor, a step that should convert the hydrophilic silanol groups to hydrophobic trimethylsilyl ethers,[25] produced films with refractive indices that were independent of relative humid-
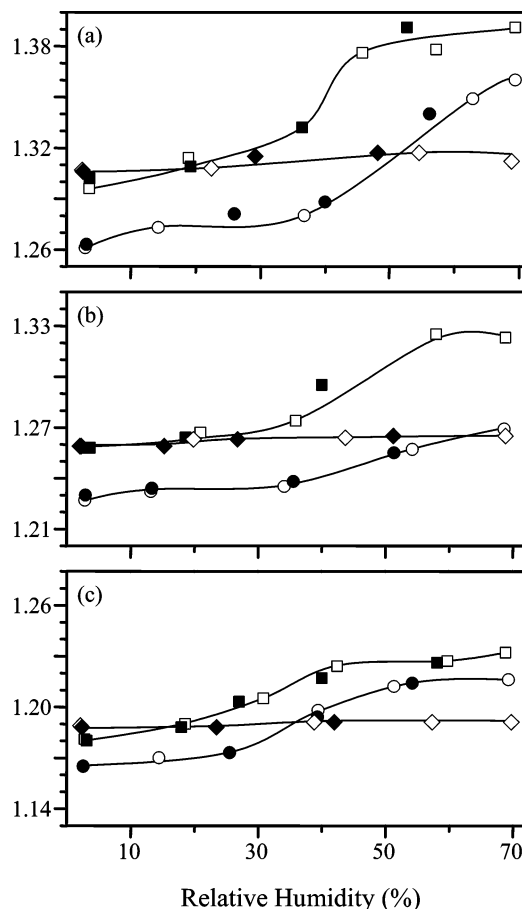
ity. After 12 h of treatment at room temperature, the calcined films were removed from the vapor and heated at 110 °C for 10 h under dynamic vacuum to remove any unreacted TMSCl or hexamethyldisiloxane byproduct. A survey XPS spectrum of a TMSCl-treated film prepared from sol A showed a pronounced increase in carbon photoemission, from 1.4% to 13.7%, relative to the spectrum obtained prior to treatment (Figure 3c). A high-resolution XPS spectrum of the Si 2p region after TMSCl treatment (Figure 9, solid line) showed a low binding energy shoulder at 101.5 eV comprising ~8% of the silicon 2p photoemission. This component was not present prior to treatment (Figure 9, dotted line) and has a binding energy consistent with that reported for the trimethylsilyl ether.[26] Treatment with trimethylchlorosilane caused the refractive indices of the films to increase to approximately the values observed before calcination (at 3% RH) and resulted in films that exhibited almost no change in index with humidity (Figures 8). The slight changes in refractive index are within the experimental error of the measurements. In addition, no change in film thickness was observed after the TMSCl treatment.

## Conclusions

Sequential adsorption of a polyelectrolyte and oligomeric species from a silica sol onto silicon substrates produces porous

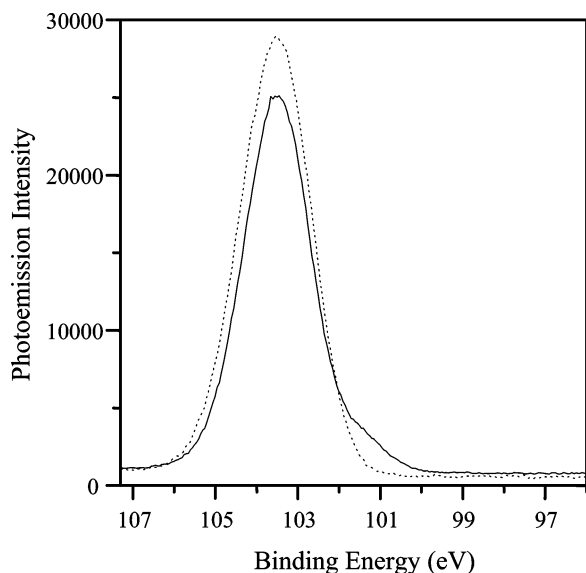(25) Plueddemann, E. P. *Silane Coupling Agents*; Plenum Press: New York, 1982.

**Figure 9.** High-resolution XPS spectra in the Si 2p region of a film prepared with sol **A**: after calcination at 500 °C in air for 10 h (dotted line), and after subsequent treatment with trimethylchlorosilane (solid line).

silica films with control over both refractive index and thickness. Films with refractive indices as low as 1.16 and containing very little organic material were obtained. Scanning electron microscopy revealed that the low refractive indices were the result of a low packing density of ~10-nm silica particles that constitute these films. Calcination reduced the amount of organic material within these films to below 2%, with only a minor decrease in film thickness, and resulted in silica with porosities of up to 67% and a refractive index as low as 1.14. The refractive indices of these films were affected by relative humidity, reflecting the hydrophilicity of the silica surface, an effect nearly eliminated by treatment with trimethylchlorosilane. In addition to the tunability of the optical path length, the porous and chemically modifiable nature of these silica films may hold promise for their use as low-dielectric materials, and as coatings for chromatographic supports.

## Experimental Section

**Materials.** Poly(diallyldimethylammonium chloride) (20% (w/w) aqueous solution, MW 200 000–350 000) was obtained from Aldrich and diluted to 0.25% (w/w) with Millipore Milli-Q water (15–16 MΩ). Absolute ethanol (McCormick), sodium hydroxide (99.99%, Aldrich), tetraethyl orthosilicate (TEOS, 98%, Acros), and trimethylchlorosilane (Aldrich, 99+%) were used as received.

Silicon (100) substrates (p-doped) were obtained from Si–Tech, Inc., cut into ~1 × ~3.0-cm pieces, swabbed with absolute ethanol to remove any silicon dust, and cleaned in piranha solution (1:2 (v/v) 30% $H_2O_2$ and concentrated $H_2SO_4$). *Caution: Piranha solution reacts violently with organic material and should be handled carefully.* The clean wafers were rinsed thoroughly with Milli-Q water and dried with nitrogen. The thickness of the native oxide on these wafers was 1.6–1.8 nm.

**Ellipsometric Analysis.** The ellipsometric data were obtained on a Rudolph Auto-EL III nulling ellipsometer with a HeNe laser ($\lambda = 632.8$ nm) at an angle of incidence of 70°. Four spots were measured at 4–7% relative humidity, unless otherwise noted, and averaged for each sample.[27] The thickness of the multilayer was determined using a

double-layer model and software supplied by the manufacturer (Program 222 on the Auto-EL III). This program utilizes the thickness and refractive index of the native oxide on silicon, as well as the refractive index of the silicon substrate, to determine the starting point for the calculation of the thickness and index of the sample film. Refractive indices were also determined for films greater than ~80-nm in thickness using the same program.[18]

**Scanning Electron Microscopy (SEM).** Scanning electron micrographs were obtained on either a JEOL 6335 or 6700 Field Emission microscopes using a secondary electron detector. Samples were uncoated, mounted on aluminum stubs, and freshly cleaved if necessary. Images obtained on the 6700 FESEM were found to be of superior quality for a number of reasons. The use of a lower beam current coupled with a more sensitive detector minimized the amount of surface charging, while still allowing image contrast. Also, the partial-in-the-lens detector used in the 6700 FESEM allowed imaging at a shorter working distance than possible with the 6335 FESEM (equipped with a standard Everhart-Thornley detector), and thus higher resolution images were obtained.

**X-ray Photoelectron Spectroscopy (XPS).** X-ray photoelectron spectroscopy was performed using a Scienta ESCA300 (Uppsala, Sweden) with monochromatic Al–Kα X-rays and at a working pressure of $10^{-9}$ mbar. Survey spectra were collected with a pass energy of 300 eV (1.0-eV steps), and high-resolution spectra were collected with a pass energy of 150 eV (0.05-eV steps). A takeoff angle between the surface of the film and the detector of 90° was used. Under our experimental conditions, peak resolution was limited by the inherent sample line width and not by instrumental factors. All spectra were referenced to the main Si 2p peak, set at 103.5 eV.[28] The following sensitivity factors determined for the Scienta ESCA300 by A. Miller were used for quantitative analysis: O 1s, 2.837; C 1s, 1.000; Si 2p 0.960; N 1s, 1.620.

**Preparation of Silica Sols.** Sols A and B were produced by adding tetraethyl orthosilicate (TEOS) to 100 mL of deionized water (pH between 6.0 and 6.5) to form a 0.01-M solution and stirring at 400 rpm (Variomag Telenodul 20P stirrer). After 2 h, an amount of aqueous sodium hydroxide was added to produce either a 35:1 (sol A) or a 175:1 (sol B) molar ratio of TEOS to base. For sol A, the concentration of the aqueous sodium hydroxide added was ~0.05 M, and for sol B it was ~0.02 M. The corresponding initial concentrations of base in these solutions were ~0.28 mM and ~0.057 mM for sol A and sol B, respectively. After it had stirred for 2 additional hours, the solution was divided into 20-mL portions that were continuously stirred at 400 rpm during aging and film formation. Sol C was prepared by adding TEOS directly to 100 mL of aqueous sodium hydroxide to form a 0.01-M solution of TEOS and having an initial molar ratio of TEOS to base of 175:1. The solution was stirred for 4 h at 400 rpm, after which it was divided into 20-mL portions that were continuously stirred at 400 rpm during aging and film formation. A solution "batch" refers to films prepared from the same initial 0.01-M TEOS solution.

**Multilayer Preparation.** A clean silicon wafer was rinsed with Milli-Q water and dried with nitrogen. The wafer was suspended vertically in the 0.25% (w/w) PDDA solution, and after 3 min it was removed, rinsed with Milli-Q water, and dried with a jet of $N_2$. Rinsing and drying was then repeated. The same process was followed using one of the silica sols, stirred at 400 rpm. An adsorption of PDDA followed by an adsorption of silica constitutes one "adsorption cycle."

**Calcination of As-Adsorbed PDDA/Silica Multilayers.** As-adsorbed multilayer films were placed film-side up on porous alumina blocks and heated in an L + L series furnace at 500 °C in air for 10 h. The furnace was heated at a rate of 5 °C/min and cooled at a rate of ~1 °C/min back to room temperature.

(26) Yang, H.-S.; Choi, S.-Y.; Hyun, S.-H.; Park, C.-G. *Thin Solid Films* **1999**, *348*, 69.
(27) Kleinfeld, E. R.; Ferguson, G. S. *Chem. Mater.* **1995**, *7*, 2327.

(28) Moulder, J. F.; Stickle, W. F.; Sobol, P. E.; Bomden, K. D. In *Handbook of X-ray Photoelectron Spectroscopy*; Chastain, J., Ed.; Perkin-Elmer: Eden Prairie, Minnesota, 1992.

**Treatment of Calcined Films with Trimethylchlorosilane.** Calcined films were placed diagonally in a 20-mL vial with the film facing toward the bottom of the vial, and a glass slide spacer was used to separate the film from the bottom of the vial. One drop ($\sim$0.01 mL) of trimethylchlorosilane (TMSCl) was placed in the bottom of the vial and then the vial was sealed under air for 12 h. To remove any unreacted TMSCl or other byproducts, the film was then placed in a VWR Scientific 1410 series vacuum oven and heated under dynamic vacuum at 110 °C for 10 h.

**Response of Films to Humid Nitrogen.** Multilayer films were exposed to various levels of RH both before and after calcination, and after TMSCl treatment. The RH was cycled between $\sim$3 % and $\sim$70 %, with ellipsometric measurements taken 5 and 10 min after the RH calibrator (Vaisala HMC 20) had equilibrated at each value of RH. The apparatus and this procedure have been described in more detail previously.[27]